# Assignment of the vibrational spectra of the parent polysilsesquioxane (POSS): Octahydridosilasequioxane, $H_8Si_8O_{12}$

Stewart F. Parker

**Published version information**

**Citation:** Parker, SF. "Assignment of the vibrational spectra of the parent polysilsesquioxane (POSS): Octahydridosilasequioxane, $H_8Si_8O_{12}$". Spectrochimica Acta Part A: Molecular and Biomolecular Spectroscopy, vol. 171 (2017): 222–228.

doi: http://dx.doi.org/10.1016/j.saa.2016.08.009

# Assignment of the vibrational spectra of the parent polysilsesquioxane (POSS): octahydridosilasequioxane, $H_8Si_8O_{12}$.

Stewart F. Parker

*ISIS Facility, STFC Rutherford Appleton Laboratory, Chilton, Didcot, OX11 0QX, UK*

Abstract

Polysilsesquioxanes (POSS) are molecules with the empirical formula $(RSiO_{1.5})_n$ where R is a hydrogen atom or hydroxyl or an organic moiety such as an alkyl, alkene, acrylate or epoxide. The silicon atoms occupy the corners of a cube and oxygen atoms are located on the edges, the versatility of silsesquioxanes arises from the vacant fourth position of silicon. The choice of substituent enables a wide variety of properties to be engineered in a straightforward manner. The parent POSS is octasilsesquioxane, $H_8Si_8O_{12}$, with R = H and $n$ = 8. The present work employs periodic density functional theory calculations in conjunction with *all* the available vibrational (infrared, Raman and inelastic neutron scattering) spectra to generate a complete assignment of all the modes of the parent POSS octasilsesquioxane and some of its isotopomers for both the free, ($O_h$), molecule and the solid state material ($C_{3i}$ site symmetry) including the forbidden and very weak modes. The latter are of interest because in less symmetrical silsesquioxanes, these modes will be activated.

## 1. INTRODUCTION

Polysilsesquioxanes (POSS) are molecules with the empirical formula $(RSiO_{1.5})_n$ where R is a hydrogen atom or hydroxyl or an organic moiety such as an alkyl, alkene, acrylate or epoxide [1], see Fig. 1. It can be seen that silicon atoms occupy the corners of a cube and oxygen atoms are located on the edges, the versatility of silsesquioxanes arises from the vacant fourth position of silicon. The choice of substituent enables a wide variety of properties to be engineered in a straightforward manner [2]. These include solubility in water or organic solvents, the ability to be blended into many polymers and, unlike most silicones or fillers, POSS molecules contain organic substituents on their outer surfaces, making them compatible or miscible with most polymers. The range of properties can be extended by choosing a reactive R substituent that can be polymerised to make true organic-inorganic hybrid polymers or eliminated to form mesoporous silicates with a well-defined cage structure. POSS molecules can thus be viewed as very small, perfectly monodisperse silica nanoparticles, with typical diameters on the order of 1−3 nm.

The parent POSS is octasilsesquioxane, $H_8Si_8O_{12}$, see Fig. 1, with R = H and $n$ = 8, and was first synthesised in very low yield in 1959 [3], more efficient routes are now available and higher POSS with $n$= 12,14,16 and 18 have also been synthesised and characterised [4]. The reactivity of $H_8Si_8O_{12}$ can be understood as occurring *via* a pentacoordinate Si intermediate and this helps explain why substitution in compounds with R = alkyl or aryl is difficult or impossible because of steric hindrance in the intermediate [5]. The solid state structure of $H_8Si_8O_{12}$ has been determined several times, the most relevant is the neutron diffraction study by Törnroos [6]. The space group is trigonal $R\bar{3}$ (no. 148), there is one molecule in the primitive unit cell that occupies a site of $C_{3i}$ symmetry. The ideal molecular symmetry is octahedral, $O_h$, and the distortion from this is small.

The vibrational spectroscopy of octasilsesquioxane has been investigated several times over the years [7-12]. The near-octahedral symmetry of the molecule means that there are many modes that are either forbidden or very weak in both the infrared and Raman spectra. To observe these modes the inelastic neutron scattering (INS) spectrum was recorded [10]. INS spectroscopy [13] is highly complementary to infrared and Raman spectroscopy, for octasilsesquioxane the attribute that there are no selection rules and all modes are allowed was the main motivation. The vibrational structure of octahedral $H_8Si_8O_{12}$ was investigated in detail, and a harmonic force field in terms of internal force constants was determined, based on infrared, FT-Raman and INS data and on a normal coordinate analysis of $H_8Si_8O_{12}$ and $D_8Si_8O_{12}$. Group frequencies were assigned according to a potential energy analysis and relations to group frequencies of comparable silicon compounds were discussed. Based on the force field, the lowest internal torsional frequency was estimated to be 41 $cm^{-1}$. [7-10].

The molecular vibrations have also been assigned by periodic density functional theory (DFT) [14]. While DFT usually provides very reliable vibrational assignments, particularly when combined with INS data (e.g. [15-19]) as was done for octamethylsilsesquioxane [20], Schutte and Pretorius [14] only considered infrared data. Furthermore, inspection of their phonon dispersion curves shows multiple imaginary modes with large energies (up to 7 THz

= 230 $cm^{-1}$) across most of the Brillouin zone. This is indicative of a major flaw in the computational work.

The purpose of the present work is to use periodic density functional theory calculations in conjunction with *all* the available vibrational (infrared, Raman and inelastic neutron scattering (INS)) spectra to generate a complete assignment of all the modes including the forbidden and very weak modes. The latter are of interest because in less symmetrical silsesquioxanes, these modes will be activated.

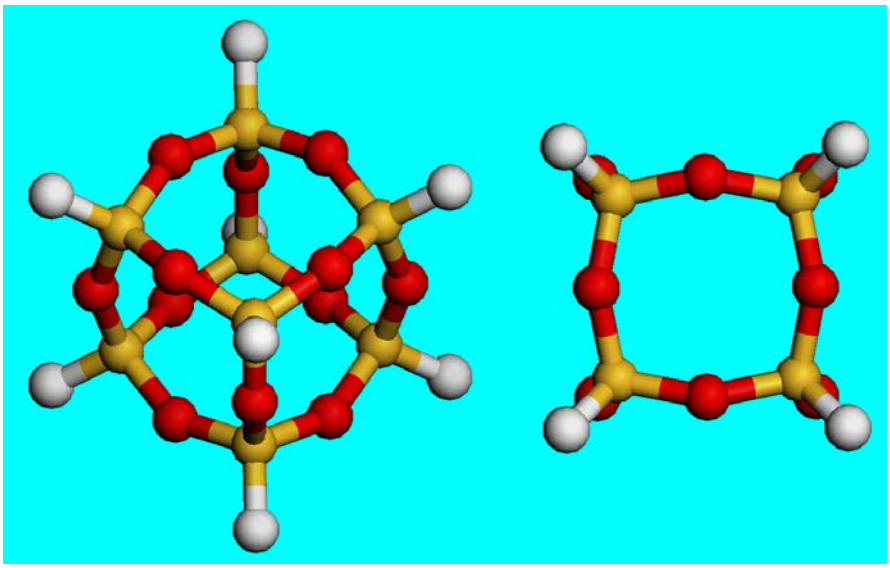

**Fig. 1.** Two views of the parent POSS, octasilsesquioxane $H_8Si_8O_{12}$, with $O_h$ symmetry. Terminal atoms are hydrogen, twofold bridging are oxygen and fourfold coordinated are silicon.

## 2. COMPUTATIONAL STUDIES

The structure of octasilsesquioxane as determined by neutron diffraction [6] was downloaded from the Inorganic Chemical Structure Database (ICSD, datacode 75244). Periodic density functional theory (periodic-DFT) calculations were carried out using the plane wave pseudopotential method as implemented in the CASTEP code [21,22]. Exchange and correlation were approximated using the PBE functional [23]. The plane-wave cut-off energy was 770 eV. Brillouin zone sampling of electronic states was performed on 3×3×1 Monkhorst-Pack grid. The equilibrium structure, an essential prerequisite for lattice dynamics calculations was obtained by BFGS geometry optimization after which the residual forces were converged to zero within ±0.0055 eV $Å^{-1}$. Phonon frequencies were obtained by diagonalisation of dynamical matrices computed using density-functional perturbation theory [24] and also to compute the dielectric response and the Born effective charges, and from these the mode oscillator strength tensor and infrared absorptivity were calculated. Raman activities were computed using a hybrid method combining density functional perturbation theory with finite displacements [24]. In addition to the calculation of transition energies and intensities at zero wavevector, phonon dispersion was also calculated along high symmetry directions throughout the Brillouin zone. For this purpose, dynamical matrices were computed on a regular grid of wavevectors throughout the Brillouin zone and Fourier interpolation was used to extend the computed grid to the desired fine set of points along the

high-symmetry paths [25]. Transition energies for isotopic species were calculated from the dynamical matrix that is stored in the CASTEP checkpoint file using the PHONONS utility [26] The atomic displacements in each mode that are part of the CASTEP output (.phonon files) are also all that is required to generate the INS spectrum using the program ACLIMAX [27]. Visualization of the modes to aid assignments was carried out with Jmol [28]. The .phonon files and a description of how to use Jmol to visualise the modes are included in the Supporting Information. The INS spectrum of octasilsesquioxane was that reported previously [10] and is available from the INS database at: http://wwwisis2.isis.rl.ac.uk/INSdatabase/.

## 3. RESULTS AND DISCUSSION

The idealised structure of the gas phase molecule is $O_h$ and this is observed experimentally by gas phase electron diffraction [29]. In the crystal the symmetry is reduced to $C_{3i}$, Table 1 shows the correlation from $O_h$ to $C_{3i}$. It can be seen that there are a large number of modes that are inactive in the free molecule, whereas all the modes are allowed by either infrared or Raman spectroscopy in the solid state. However, a mode may be allowed but have vanishingly small intensity, this may be expected to be the case for the free-molecule forbidden modes that are activated in the solid state. Note that all the modes are allowed for INS spectroscopy

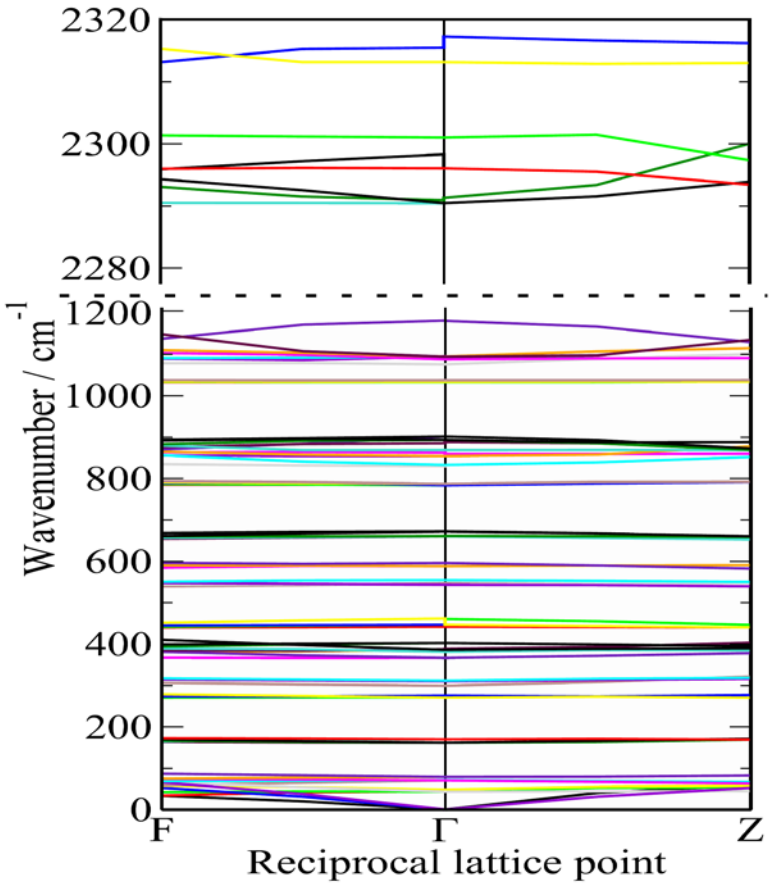


**Fig. 2.** Calculated dispersion curves for the primitive unit cell of octasilsesquioxane showing all real modes across the entire Brillouin zone. Note the change of scale at 1200 $cm^{-1}$. The data have not been scaled.

Fig. 2 shows the dispersion curves calculated for the solid state structure of octasilsesquioxane. In contrast to [14], the modes are all real across the entire Brillouin zone, as expected for a stable structure. (The discontinuities at the Γ-point are due to longitudinal optical transverse optical (LOTO) splitting).

Fig. 3 compares the experimental INS spectrum of octasilsesquioxane [10], 3a, with that generated from the calculation of the free molecule with $O_h$ symmetry, 3b, and the full dispersion calculation of the solid state structure, 3c. (In both 3b and 3c, the region 0 – 2000 $cm^{-1}$ has been scaled by 1.03). It can be seen that both structures fit the data very well, thus validating the calculations. As would be expected, the match of the experimental data to the solid state structure is marginally better, particularly in the lattice mode region.

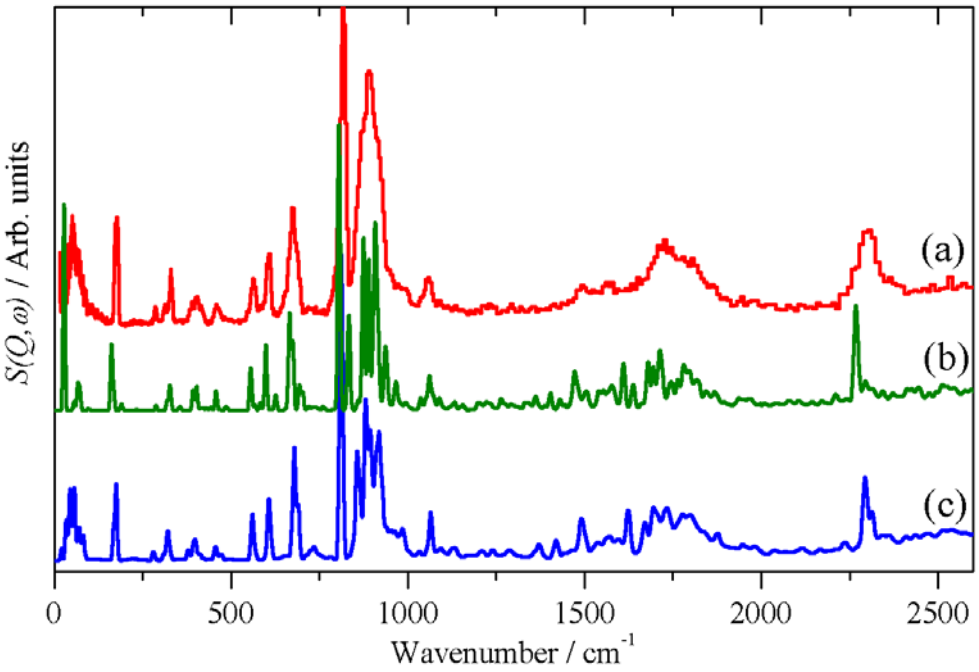


**Fig. 3.** Comparison of: (a) the experimental INS spectrum of octasilsesquioxane [10] and that generated from the CASTEP calculation of (b) the free molecule with $O_h$ symmetry and (c) the solid state with $C_{3i}$ site symmetry. In (b) and (c) the 0 – 2000 $cm^{-1}$ region has been scaled by 1.03.

Table 2 lists the observed and calculated transition energies and intensities for the free molecule and the solid state. The splitting of the *T* modes into *A* and *E* components by the reduction in the molecular symmetry from $O_h$ to $C_{3i}$ is visible for most of the modes in the infrared spectrum, *e.g.* 875 ($T_{1u}$) → 882 ($E_u$) and 861 ($A_u$) $cm^{-1}$. It is noted that the calculated infrared intensity of the $E_u$ modes is approximately twice that of the $A_u$ modes, as suggested in [11], validating their assignments of the $E_u$ and $A_u$ components.

It was proposed [11] that the infrared active modes fall into two classes that depend on whether the motion is largely tangential or radial. The correlation crucially depends on whether modes 27 and 29 are described as radial and tangential respectively, as suggested in [11], or tangential and radial respectively as assigned previously [7-10]. (The mode

numbering is that used previously [7-11] and is given in Table S1 of the Supplementary Information). As may be seen from Fig. 4, neither description is accurate, in both cases the silicon and hydrogen atoms on the threefold axis move radially, while the other atoms move tangentially. The difference in the modes is the relative phases of the motions. (Animations of the modes can be seen using Jmol [28], see the Supplementary Information for details).

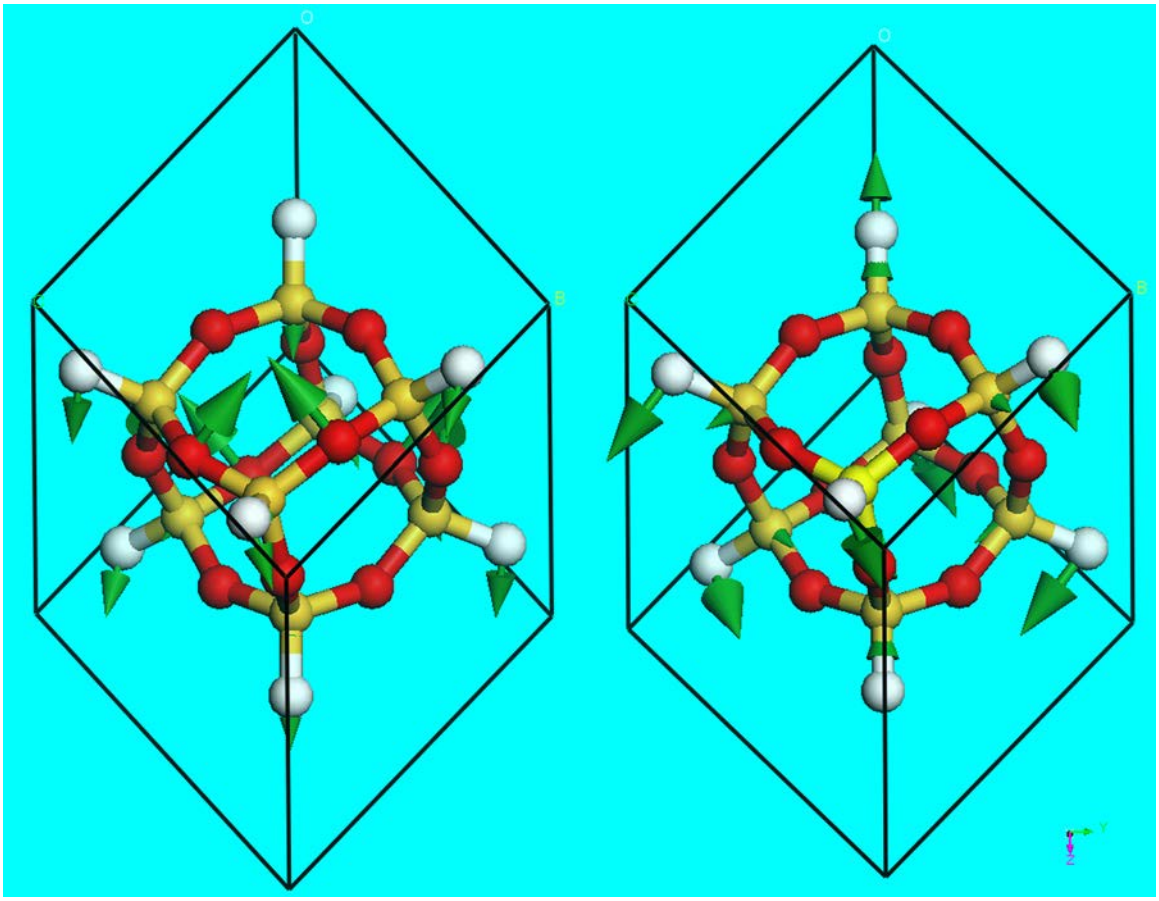

**Fig. 4.** Displacements of the atoms in the $A_u$ component of modes 27 (left) and 29 (right). Terminal atoms are hydrogen, twofold bridging are oxygen and fourfold coordinated are silicon.

Experimental data is available for most of the infrared and Raman active modes of $D_8Si_8O_{12}$ and a few of the modes of $HD_7Si_8O_{12}$ (present as an impurity in $D_8Si_8O_{12}$) [8,9]. For $HD_7Si_8O_{12}$ as a free molecule (*i.e.* $O_h$ symmetry in the $H_8$ or $D_8$ parent), there is only one isotopomer because all the sites are identical under $O_h$ symmetry. This has $C_{3v}$ symmetry and the correlation is given in Table 1. For the solid state $C_{3i}$ species, there are two isotopomers depending on whether the Si–H is bond lies along the threefold axis or not, these have $C_3$ and $C_1$ site symmetry respectively. The correlation for the $C_3$ species is the same as for $C_{3i}$ except that the *g* and *u* subscripts are omitted (since the centre of symmetry is destroyed by the isotopic substitution) and all modes are allowed in both the infrared and Raman spectrum, as is also the case for $C_1$ site symmetry. CASTEP allows the ready calculation of isotopomers *via* the PHONONS utility [26] and the results are given in Table 3. It can be seen that the agreement is generally excellent.

## 4. CONCLUSIONS

This study provides a complete assignment of the vibrational spectra of the parent POSS octasilsesquioxane and some of its isotopomers for both the free, ($O_h$), molecule and the solid state material ($C_{3i}$ site symmetry). The combination of infrared, Raman and INS spectroscopic data from the literature has enabled most of the modes to be observed.


### Acknowledgements

The STFC Rutherford Appleton Laboratory is thanked for access to neutron beam facilities. Computing resources (time on the SCARF compute cluster for the CASTEP calculations) was provided by STFC's e-Science facility. The use of the Inorganic Chemical Structure Database (ICSD) *via* the EPSRC funded National Chemical Database Service hosted by the Royal Society of Chemistry is acknowledged.


### References


1) S.-W. Kuoa and F.-C. Chang, Prog. Pol. Sci. 36 (2011) 1649–1696.
2) D. B. Cordes, P. D. Lickiss and F. Rataboul, Chem. Rev. 110 (2010) 2081–2173.
3) R. Müller, F. Köhne and S. Sliwinski, J. Prakt. Chem. 9 (1959) 71-74.
4) P. A. Agaskar and W. Klemperer, Inorg. Chim. Acta 229 (1995) 355–364.
5) G. Calzaferri and R. Hoffmann, J. Chem. Soc. Dalton Trans. (1991) 917-928.
6) K. W. Törnroos, Acta Cryst. C 50 (1994) 1646–1648.
7) P. Bornhauser and G. Calzaferri, Spec. Acta 46A (1990) 1045-1056.
8) M. Bärtsch, P. Bornhauser, H. Bürgy and G. Calzaferri, Spec. Acta 47A (1991) 1627-1629.
9) M. Bärtsch, P. Bornhauser, G. Calzaferri and R. Imhof, J. Phys. Chem. 98 (1994) 2817.
10) C. Marcolli, P. Lainé, R. Bühler, G. Calzaferri and J. Tomkinson, J. Phys. Chem. B 101 (1997) 1171-1179.
11) A. M. Chomel, U. A. Jayasooriya and F. Babonneau, Spec. Acta 60A (2004) 1609-1616.
12) P. G. Harrison and C. Hall, Main Group Chemistry 20 (2011) 515-529.
13) P.C.H. Mitchell, S.F. Parker, A.J. Ramirez-Cuesta, J. Tomkinson, Vibrational Spectroscopy With Neutrons, With Applications in Chemistry, Biology, Materials Science and Catalysis, World Scientific, Singapore, 2005.
14) C. J. H. Schutte and J. A. Pretorius, Proc. R. Soc. A468 (2012) 851–870.
15) F. Fontaine-Vive, M.R. Johnson, G.J. Kearley, J.A.K. Howard and S.F. Parker, J. Amer. Chem. Soc. 128 (2006) 2963-2969.
16) G.D. Barrerra, S.F. Parker, A.J. Ramirez-Cuesta, and P.C.H. Mitchell, Macromolecules, 39 (2006) 2683-2690.
17) A. Lovell, F. Fernandez-Alonso, N.T. Skipper, K. Refson, S.M. Bennington and S.F. Parker, Phys. Rev. Lett., 101, (2008) 126101.
18) D.I. Kolokolov, H. Jobic, A.G. Stepanov, M. Plazanet, M. Zbiri, J. Ollivier, V. Guillerm, T. Devic, C. Serre and G. Férey, Eur. Phys. J.-Special Topics 189 (2010) 263-271.

19) C.E. White, G.J. Kearley, J.L. Provis and D.P. Riley, J. Chem. Phys. 128 (2013) 194501.
20) N. Jalarvo, O. Gourdon, G. Ehlers, M. Tyagi, S. K. Kumar, K. D. Dobbs, R. J. Smalley, W. E. Guise, A. J. Ramirez-Cuesta, C. Wildgruber and M. K. Crawford, J. Phys. Chem. C 118 (2014) 5579−5592.
21) S. J. Clark, M. D. Segall, C. J. Pickard, P. J. Hasnip, M. J. Probert, K. Refson, and M. C. Payne, Z. Krist. **220**, 567 (2005).
22) K. Refson, P. R. Tulip, and S. J. Clark, Phys. Rev. B **73**, 155114 (2006).
23) J. Perdew, K. Burke, and M. Ernzerhof, Phys. Rev. Lett. **77**, 3865 (1996).
24) V. Milman, A. Perlov, K. Refson, S. J. Clark, J. Gavartin, and B. Winkler, J. Phys.: Condens. Matter **21**, 485404 (2009).
25) X. Gonze, J.-C. Charlier, and M. P. Teter, Phys. Rev. B **50**, 13035-13038 (1994).
26) K. Refson, *Phonons and Related Calculations in CASTEP*, http://www.castep.org/
27) A. J. Ramirez-Cuesta, Comput. Phys. Commun. **157**, 226 (2004).
28) Jmol: an open-source Java viewer for chemical structures in 3D. http://www.jmol.org/
29) D. A. Wann, R. J. Less, F. Rataboul, P. D. McCaffrey, A. M. Reilly, H. E. Robertson, P. D. Lickiss and D. W. H. Rankin, Organometallics, 27 (2008) 4183–4187.

Table 1: Correlation diagram and spectral activity for octasilsesquioxane from the free molecule, $O_h$, to the site group, $C_{3i}$, and also for the $HD_7Si_8O_{12}$ isotopomer. Note that *all* modes are allowed for INS spectroscopy.

| $H_8Si_8O_{12}$ | | $HD_7Si_8O_{12}$ | | Primitive cell of space group $R\bar{3}$ | |
|---|---|---|---|---|---|
| $O_h$ | Activity[a] | $C_{3v}$ | Activity | Site group $C_{3i}$ | Activity |
| Si–H stretches | | | | | |
| $A_{1g}$ | R | $A_1$ | IR/R | $A_g$ | R |
| $T_{2g}$ | R | $A_1 + E$ | IR/R | $A_g + E_g$ | R |
| $A_{2u}$ | ia | $A_1$ | IR/R | $A_u$ | IR |
| $T_{1u}$ | IR | $A_1 + E$ | IR/R | $A_u + E_u$ | IR |
| Framework + Si–H bending | | | | | |
| $2\,A_{1g}$ | R | $2\,A_1$ | IR/R | $2\,A_g$ | R |
| $1\,A_{2g}$ | ia | $1\,A_2$ | ia | $1\,A_g$ | IR |
| $4\,E_g$ | R | $4\,E$ | IR/R | $4\,E_g$ | R |
| $3\,T_{1g}$ | ia | $3\,A_2 + 3\,E$ | ia & IR/R | $3\,A_g + 3\,E_g$ | IR |
| $5\,T_{2g}$ | R | $5\,A_1 + E$ | IR/R | $5\,A_g + 5\,E_g$ | R |
| $2\,A_{2u}$ | ia | $2\,A_1$ | IR/R | $2\,A_u$ | IR |
| $3\,E_u$ | ia | $3\,E$ | IR/R | $3\,E_u$ | IR |
| $5\,T_{1u}$ | IR | $5\,A_1 + 5\,E$ | IR/R | $5\,A_u + 5\,E_u$ | IR |
| $4\,T_{2u}$ | ia | $4\,A_2 + 4\,E$ | ia & IR/R | $4\,A_u + 4\,E_u$ | IR |
| Libration | | | | | |
| | ia | | ia | $A_g + E_g$ | R |
| Translation | | | | | |
| | ia | | ia | $A_u + E_u$ | IR |

[a]IR = infrared allowed, R = Raman allowed, IR/R infrared and Raman allowed, ia = inactive in both infrared and Raman.

Table 2: Observed and calculated vibrational transition energies and intensities of octasilsesquioxane for the free molecule with $O_h$ symmetry and the solid state material with $C_{3i}$ symmetry.

| Free molecule, $O_h$ | | | | | | Solid state, $C_{3i}$ | | | | | | | Description[a] |
|---|---|---|---|---|---|---|---|---|---|---|---|---|---|
| CASTEP[b] | | | | Expt | | CASTEP[b] | | | | Expt | | | |
| Sym | cm$^{-1}$ | IR / km mol$^{-1}$ | R / Å$^4$ amu$^{-1}$ | IR [10] / cm$^{-1}$ | R [7] / cm$^{-1}$ | Sym | cm$^{-1}$ | IR / km mol$^{-1}$ | R / Å$^4$ amu$^{-1}$ | IR [11] / cm$^{-1}$ | R [10] / cm$^{-1}$ | INS [10] / cm$^{-1}$ | |
| $A_{1g}$ | 2274 | | 1105 | | (2302) | $A_g$ | 2383 | | 1606 | | 2302 | | νs(Si–H) |
| $T_{1u}$ | 2269 | 852 | | 2277 m | | $A_u$ | 2382 | 315 | | 2293 | | 2300 | νas(Si–H) |
| | | | | | | $E_u$ | 2365 | 752 | | 2274 | | | |
| $T_{2g}$ | 2267 | | 589 | | (2286) | $A_g$ | 2370 | | 1948 | | 2296 | | νas(Si–H) |
| | | | | | | $E_g$ | 2359 | | 295 | | 2286 | | |
| $A_{2u}$ | 2265 | | | | | $A_u$ | 2359 | 56 | | | | | νas(Si–H) |
| $T_{1u}$ | 1156 | 5835 | | 1141 vs | | $A_u$ | 1129 | 2792 | | 1120 | | | νas(Si–O) |
| | | | | | | $E_u$ | 1127 | 5892 | | 1183 | | | |
| $T_{2g}$ | 1147 | | | | (1118) | $E_g$ | 1127 | | 8 | | 1117 | | νas(Si–O) |

| | | | | | | | | | | | | |
|---|---|---|---|---|---|---|---|---|---|---|---|---|
| | | | | | | $A_g$ | 1121 | | 6 | | | |
| $A_{2u}$ | 1120 | | | | | $A_u$ | 1108 | 41 | | | | ν as(Si–O) |
| $T_{1g}$ | 1061 | | | | | $A_g$ | 1068 | | 1 | | 1058 | ν as(Si–O) |
| | | | | | | $E_g$ | 1064 | | | | | |
| $E_u$ | 1060 | | | | | $E_u$ | 1065 | 12 | | | | ν as(Si–O) |
| $E_g$ | 912 | | 21 | | (932) | $E_g$ | 929 | | 35 | 932 | 932 | δ(Si-O-H) |
| $T_{2u}$ | 907 | | | | | $E_u$ | 920 | 16 | | | 915 | δ(Si-O-H) |
| | | | | | | $A_u$ | 909 | 110 | | | | |
| $T_{2g}$ | 889 | | 72 | | (897, 883) | $A_g$ | 895 | | 35 | 897 | | δ(Si-O-H) |
| | | | | | | $E_g$ | 880 | | 21 | 893 | 889 | |
| $T_{1u}$ | 875 | 1443 | | 881 s | | $E_u$ | 858 | 2514 | 882 | | 868 | δ(Si-O-H) |
| | | | | | | $A_u$ | 852 | 1346 | 861 | | | |
| $E_u$ | 806 | | | | | $E_u$ | 811 | 3 | | | 817 | δ(Si-O-H) |
| $T_{1g}$ | 805 | | | | | $A_g$ | 811 | | 1 | 811 | | δ(Si-O-H) |
| | | | | | | $E_g$ | 807 | | 1 | | 817 | |

| | | | | | | | | | | | | | | |
|---|---|---|---|---|---|---|---|---|---|---|---|---|---|---|
| $E_g$ | 675 | | 44 | | (697) | $E_g$ | 692 | | 95 | | 697 | 688 | νs(Si–O) |
| $T_{2u}$ | 666 | | | | | $E_u$ | 681 | 10 | | | | 675 | νs(Si–O) |
| | | | | | | $A_u$ | 680 | 3 | | | | | |
| $T_{2g}$ | 599 | | | | | $A_g$ | 614 | | 2 | | 610 | | νs(Si–O) |
| | | | | | | $E_g$ | 606 | | 1 | | | 607 | |
| $A_{1g}$ | 568 | | 12 | | (579) | $A_g$ | 571 | | 52 | | 580 | | δ(O–Si–O) |
| $T_{1u}$ | 556 | 57 | | 566 w | | $A_u$ | 563 | 13 | | 568 | | | δ(O–Si–O) |
| | | | | | | $E_u$ | 560 | 12 | | 557 | | 564 | |
| $T_{1u}$ | 457 | 381 | | 465 m | | $A_u$ | 460 | 222 | | 483 | | | δ(O–Si–O) |
| | | | | | | $E_u$ | 460 | 534 | | 463 | | 459 | |
| $A_{1g}$ | 443 | | 56 | | (456) | $A_g$ | 455 | | 184 | | 456 | | δ(O–Si–O) |
| $E_g$ | 413 | | | | | $E_g$ | 415 | | 2 | | 423 | 418 | δ(O–Si–O) |
| $T_{2g}$ | 403 | | | | (411) | $E_g$ | 398 | | 2 | | 414 | 403 | δ(O–Si–O) |
| | | | | | | $A_g$ | 393 | | 3 | | | | |
| $T_{1u}$ | 393 | 435 | | 399 s | | $A_u$ | 378 | 448 | | 400 | | | δ(O–Si–O) |

| | | | | | | | | | |
|---|---|---|---|---|---|---|---|---|---|
| | | | $E_u$ | 378 | 814 | | 389 | | 387 | |
| $T_{1g}$ | 328 | | $A_g$ | 321 | | | | 352 | 329 | δ(O–Si–O) |
| | | | $E_g$ | 319 | | | | | 312 | |
| $A_{2u}$ | 319 | | $A_u$ | 309 | 10 | | | | | δ(O–Si–O) |
| $T_{2u}$ | 287 | | $A_u$ | 284 | 9 | | | | | δ(O–Si–O) |
| | | | $E_u$ | 279 | 1 | | | | 286 | |
| $T_{2g}$ | 167 | (171) | $A_g$ | 167 | | 4 | | 171 | 175 | δ(O–Si–O) |
| | | | Eg | 167 | | 4 | | | 171 | |
| $E_u$ | 162 | | $E_u$ | 175 | | | | | | δ(O–Si–O) |
| $E_g$ | 73 | (84) | $E_g$ | 82 | | 1 | | 84 | 87 | δ(O–Si–O) |
| $T_{2u}$ | 67 | | $A_u$ | 74 | | | | | 65 | δ(O–Si–O) |
| | | | $E_u$ | 73 | | | | | | |
| $A_{2g}$ | 57 | | $A_g$ | 50 | | | | | 55 | τ(O–Si–O) |
| | | | $A_g$ | 46 | | | | | 53 | Libration |
| | | | $E_g$ | 45 | | | | | | |

| | | |
|---|---|---|
| $E_u$ | 0 | Acoustic mode |
| $A_u$ | 0 | |

[a] For both the $O_h$ and $C_{3i}$ structures visualisation of the modes is possible with the use of Jmol. See the Supporting Information for details.

[b] The modes at <2000 $cm^{-1}$ have been scaled by 1.03

Table 3: Observed and calculated vibrational transition energies and intensities of isotopomers of octasilsesquioxane for the free molecule with $O_h$ symmetry and the solid state material with $C_{3i}$ symmetry.

| Free molecule | | | | | | Solid state | | | | | | | Description[a] |
|---|---|---|---|---|---|---|---|---|---|---|---|---|---|
| CASTEP $O_h$ | | Expt | CASTEP $C_{3v}$ | | Expt | CASTEP $C_{3i}$ | | Expt | CASTEP $C_3$ | | $C_1$ | Expt | |
| D8 | | | HD7 | | | D8 | | | HD7 | | HD7 | | |
| Sym | cm$^{-1}$ | IR [7,8] / cm$^{-1}$ | Sym | cm$^{-1}$ | IR [8] / cm$^{-1}$ | Sym | cm$^{-1}$ | R [8] / cm$^{-1}$ | Sym | cm$^{-1}$ | cm$^{-1}$ | R [8] / cm$^{-1}$ | |
| $A_{1g}$ | 1693 | | $A_1$ | 2277 | | $A_g$ | 1759 | 1676 | $A$ | 2374 | 2322 | 2301<br>2292 | νs(Si–D/H) |
| $T_{1u}$ | 1688 | 1658 | $A_1$ | 1693 | | $A_u$ | 1759 | | $A$ | 1759 | 1726 | | νas(Si–D) |
| | | | $E$ | 1688 | | $E_u$ | 1721 | | $E$ | 1721 | 1759<br>1759 | | |
| $T_{2g}$ | 1686 | | $A_1$ | 1687 | | $A_g$ | 1727 | 1668 | $A$ | 1728 | 1721 | | νas(Si–D) |
| | | | $E$ | 1686 | | $E_g$ | 1717 | 1660 | $E$ | 1717 | 1717<br>1717 | | |
| $A_{2u}$ | 1684 | | $A_1$ | 1685 | | $A_u$ | 1716 | | $A$ | 1717 | 1719 | | νas(Si–D) |

| | | | | | | | | | | | | | |
|---|---|---|---|---|---|---|---|---|---|---|---|---|---|
| $T_{1u}$ | 1155 | 1140 | $E$ | 1154 | | $E_u$ | 1118 | | $E$ | 1123 | 1123<br>1123 | | νas(Si–O) |
| | | | $A_1$ | 1154 | | $A_u$ | 1116 | | $A$ | 1118 | 1119 | | |
| $T_{2g}$ | 1146 | | $A_1$ | 1146 | | $E_g$ | 1123 | | $E$ | 1119 | 1118<br>1118 | | νas(Si–O) |
| | | | $E$ | 1145 | | $A_g$ | 1117 | 1115 | $A$ | 1116 | 1116 | | |
| $A_{2u}$ | 1119 | | $A_1$ | 1118 | | $A_u$ | 1101 | | $A$ | 1101 | 1101 | | νas(Si–O) |
| $T_{1g}$ | 1041 | | $E$ | 1048 | | $A_g$ | 1044 | | $A$ | 1044 | 1051 | | νas(Si–O) |
| | | | $A_2$ | 1041 | | $E_g$ | 1042 | | $E$ | 1050 | 1049<br>1043 | | |
| $E_u$ | 1040 | | $E$ | 1039 | | $E_u$ | 1042 | | $E$ | 1042 | 1042<br>1042 | | νas(Si–O) |
| $E_g$ | 801 | | $E$ | 878 | 881 | $E_g$ | 817 | | $E$ | 872 | 884<br>876 | 885<br>877 | δ(Si-O-D/H) |
| $T_{2u}$ | 789 | | $E$ | 797 | 839 | $E_u$ | 802 | | $E$ | 811 | 812<br>809 | | δ(Si-O-D) |
| | | | $A_2$ | 789 | | $A_u$ | 795 | | $A$ | 795 | 800 | | |
| $T_{2g}$ | 724 | | $E$ | 765 | 770 | $A_g$ | 729 | 729 | $A$ | 730 | 716 | 764 | δ(Si-O-D) |
| | | | $A_1$ | 724 | 720 | $E_g$ | 711 | 713 | $E$ | 769 | 774 | | |

| | | | | | | | | | | | |
|---|---|---|---|---|---|---|---|---|---|---|---|
| | | | | | | | | | | 765 | |
| $T_{1u}$ | 683 | 687 | $E$ | 707 | 710 | $A_u$ | 670 | | $A$ | 670 | 660 | δ(Si-O-D) |
| | | | $A_1$ | 684 | | $E_u$ | 659 | | $E$ | 696 | 702<br>694 | |
| $E_u$ | 606 | | $E$ | 651 | 658 | $E_u$ | 607 | | $E$ | 645 | 649<br>640 | δ(Si-O-D) |
| $T_{1g}$ | 605 | | $E$ | 606 | | $A_g$ | 607 | | $A$ | 607 | 604 | δ(Si-O-D) |
| | | | $A_2$ | 605 | | $E_g$ | 603 | | $E$ | 606 | 607<br>606 | |
| $E_g$ | 548 | | $E$ | 570 | | $E_g$ | 563 | 562 | $E$ | 581 | 585<br>578 | νs(Si–O) |
| $T_{2u}$ | 546 | | $A_1$ | 562 | | $E_u$ | 560 | | $E$ | 561 | 564<br>562 | νs(Si–O) |
| | | | $E$ | 547 | | $A_u$ | 566 | | $A$ | 567 | 560 | |
| $T_{2g}$ | 528 | | $A_2$ | 546 | | $A_g$ | 558 | 541 | $A$ | 559 | 559 | νs(Si–O) |
| | | | $E$ | 532 | | $E_g$ | 548 | | $E$ | 551 | 548<br>549 | |
| $A_{1g}$ | 561 | | $A_1$ | 529 | | $A_g$ | 546 | 579 | $A$ | 547 | 553 | δ(O–Si–O) |
| $T_{1u}$ | 522 | 531 | $A_1$ | 524 | | $A_u$ | 525 | | $A$ | 526 | 527 | δ(O–Si–O) |

| | | | | | | | | | | |
|---|---|---|---|---|---|---|---|---|---|---|
| | | | $E$ | 523 | $E_u$ | 534 | | $E$ | 535 | 535<br>536 | |
| $T_{1u}$ | 447 | | $E$ | 449 | $A_u$ | 464 | | $A$ | 473 | 473 | δ(O–Si–O) |
| | | | $A_1$ | 448 | $E_u$ | 466 | | $E$ | 466 | 466<br>466 | |
| $A_{1g}$ | 440 | | $A_1$ | 441 | $A_g$ | 473 | 452 | $A$ | 464 | 464 | δ(O–Si–O) |
| $E_g$ | 413 | | $E$ | 412 | $E_g$ | 416 | | $E$ | 417 | 417<br>417 | δ(O–Si–O) |
| $T_{2g}$ | 395 | | $E$ | 397 | $E_g$ | 405 | | $E$ | 405 | 405<br>405 | δ(O–Si–O) |
| | | | $A_1$ | 396 | $A_g$ | 401 | 405 | $A$ | 402 | 401 | |
| $T_{1u}$ | 386 | 391 | $E$ | 385 | $A_u$ | 379 | | $E$ | 384 | 384<br>383 | δ(O–Si–O) |
| | | | $A_1$ | 384 | $E_u$ | 383 | | $A$ | 379 | 380 | |
| $T_{1g}$ | 322 | | $E$ | 321 | $A_g$ | 313 | 351 | $A$ | 314 | 315 | δ(O–Si–O) |
| | | | $A_2$ | 320 | $E_g$ | 305 | | $E$ | 306 | 306<br>305 | |
| $A_{2u}$ | 314 | | $A_1$ | 314 | $A_u$ | 302 | | $A$ | 302 | 302 | δ(O–Si–O) |
| $T_{2u}$ | 287 | | $A_2$ | 286 | $A_u$ | 279 | | $A$ | 279 | 280 | δ(O–Si–O) |

| | | | | | | | | | | |
|---|---|---|---|---|---|---|---|---|---|---|
| | | $E$ | 286 | $E_u$ | 271 | | $E$ | 271 | 271<br>271 | |
| $T_{2g}$ | 166 | $E$ | 166 | $A_g$ | 166 | 170 | $A$ | 166 | 166<br>166 | δ(O–Si–O) |
| | | $A_1$ | 166 | Eg | 166 | | $E$ | 166 | 166 | |
| $E_u$ | 156 | $E$ | 154 | $E_u$ | 173 | | $E$ | 174 | 174<br>174 | δ(O–Si–O) |
| $E_g$ | 73 | $E$ | 75 | $E_g$ | 101 | 84 | $E$ | 101 | 101<br>101 | δ(O–Si–O) |
| $T_{2u}$ | 66 | $A_2$ | 64 | $A_u$ | 104 | | $A$ | 104 | 103 | δ(O–Si–O) |
| | | $E$ | 63 | $E_u$ | 101 | | $E$ | 101 | 101<br>101 | |
| $A_{2g}$ | 57 | $A_2$ | 39 | $A_g$ | 101 | | $A$ | 101 | 101 | τ(O–Si–O) |
| | | | | $A_g$ | 52 | | $A$ | 52 | 52 | Libration |
| | | | | $E_g$ | 53 | | $E$ | 53 | 53 | |
| | | | | $E_u$ | | | | | | Acoustic mode |
| | | | | $A_u$ | 0 | | | | | |

[a] The modes at <2000 $cm^{-1}$ have been scaled by 1.03